Optical properties of CrO_2 and MoO_2 from 0.1 to 6 eV†

L. L. Chase
Indiana University, Bloomington, Indiana 47401
(Received 25 March 1974)

The reflectivities of single crystals of MoO_2 and oriented films of CrO_2 grown on rutile substrates have been measured from 0.1 to 6 eV. A Kramers-Kronig analysis has been performed to obtain the dielectric functions and optical conductivities. A rise in the absorption coefficient above 1.7 eV for CrO_2 and 3 eV for MoO_2 suggests that these energies separate the highest oxygen $2p$ levels from the Fermi level in the cation d bands. The conduction-electron response is fit by $m^*/m_e \sim 10$ for CrO_2 and ~ 5 for MoO_2, assuming one carrier per cation. A peak in the optical conductivity at 0.8 eV in both materials is compared with similar features in VO_2 and V_2O_3. A possible interpretation of these peaks is discussed based on a recent calculation of the optical conductivity using the Hubbard model. If this interpretation is valid, an estimate may be made of the intraion Coulomb energy, $U_c \sim 0.8$ eV.

I. INTRODUCTION

The dioxides of the $3d$, $4d$, and $5d$ transition series comprise the largest class of oxides with similar crystal structures and having a wide range of conduction properties. Two members of this series, VO_2 and NbO_2, have insulator-metal phase transitions, which have been studied extensively in recent years. One of the important properties of these oxides that is still not firmly established is their band structure, particularly the structure of the d bands. Although a modified orthogonalized plane-wave (OPW) calculation has been performed recently[1] for the $2p$ and $3d$ bands of the semiconducting and metallic phases of VO_2, the effects of electronic correlations and electron-phonon coupling, which may be crucial to understanding conduction properties, have been largely unexplored. The work reported here on CrO_2 and MoO_2 is intended mainly for comparison with the previous optical investigations of both phases of VO_2.[2-6] CrO_2 and MoO_2 have metallic conductivities similar to that of metallic VO_2. CrO_2 has the rutile structure of metallic VO_2, a $3d^2$ cation configuration, and is ferromagnetic below about 120 °C with a magnetic moment per cation corresponding to the alignment of both $3d$ electrons per cation. MoO_2 has a monoclinic structure, similar to that of semiconducting VO_2, and the Mo^{4+} have a $4d^2$ configuration. Whereas there is considerable evidence for a band overlap in VO_2, the monoclinic structure of MoO_2 and the ferromagnetic band splittings in CrO_2 should lead to conduction only in the lower π-bonded d bands of the rutile structure.

II. EXPERIMENTAL TECHNIQUES

Single crystals of MoO_2 were grown using a vapor transport process described previously.[7] Powder diffraction data on several of the crushed samples revealed the presence of no phases other than monoclinic MoO_2. As the maximum dimension of the MoO_2 crystals was about 2 mm, no attempt was made to study the reflectivity of oriented single crystals. The largest faces of several samples were mechanically polished with 0.05-μm corundum for the measurements, which were performed in air.

Oriented films of CrO_2 were deposited on (100) and (110) faces of a TiO_2 substrate by a high-pressure decomposition process.[7] From five to ten successive layers, each a few microns thick, were deposited to build up a layer about 20 μm thick. This film was then polished with submicron-size corundum. The final surface finish had a slight dullness when observed at large angles of incidence, which is probably caused by the formation of a network of oriented CrO_2 facets of microscopic size.[8] The effects of this imperfect surface on the measurements are discussed in Sec. III.

The polarized reflectivity measurements were carried out point by point over the region from 0.2 μm to above 20 μm at 15° angle of incidence using a Spex Industries model 1500 spectrometer, deuterium, tungsten, and globar sources, and phototube and thermopile detectors. A two-mirror three-reflection reference path was used in collecting the data. Calibration was made by interchanging mirrors between calibrations so that the individual mirror reflectivities were determined at each wavelength. The mirrors were checked for uniformity of reflectance over their areas and a maximum 3% variation was observed, mainly for $\lambda < 3000$ Å.

III. EXPERIMENTAL RESULTS

The reflectivities of CrO_2 and MoO_2 at 300 °K are shown in Figs. 1 and 2, respectively. The energy resolution of the data was better than 0.03 eV. Although the MoO_2 data are for an unoriented sample, polarized measurements were performed to eliminate distortions of the spectrum caused by the wavelength-dependent polarization of the spectrometer output. The CrO_2 data are corrected for dif-

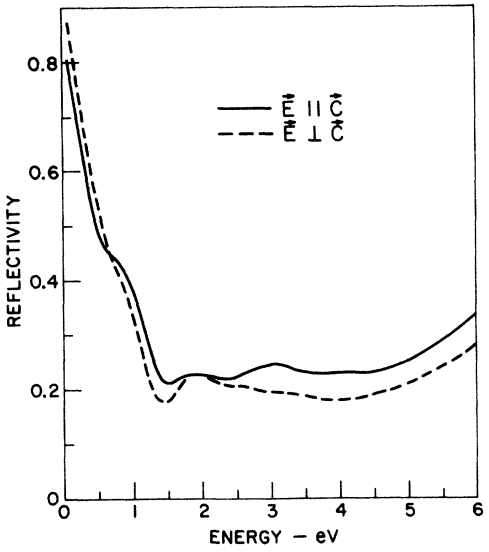

FIG. 1. Reflectivity of CrO_2 at 300 °K, corrected for scattering as discussed in the text.

fuse reflection as discussed below. A Kramers-Kronig transformation was made on the data to obtain the dielectric functions and conductivities of both materials. The standard method was used to correct for the cutoff of the data above $E_m = 6$ eV by assuming $R = R_m(E_m/E)^p$ for $E > E_m$. The parameter p was obtained by a least-squares fit to the optical constants n, k determined from the angular dependence of the reflectivity R_p for light polarized in the plane of incidence. These latter measurements were carried out using argon and helium-neon laser lines and were least-squares fit to the expression

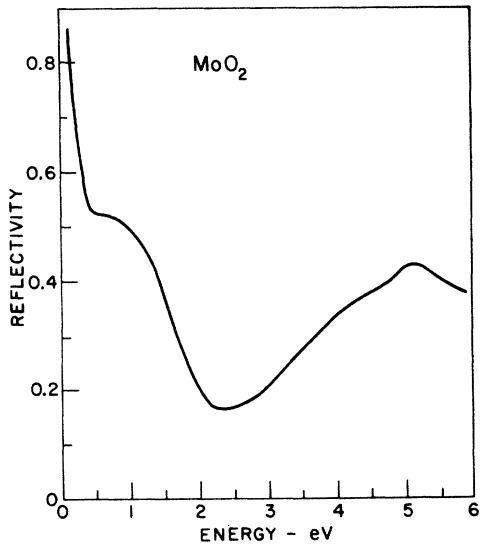

FIG. 2. Reflectivity of MoO_2 at 300 °K.

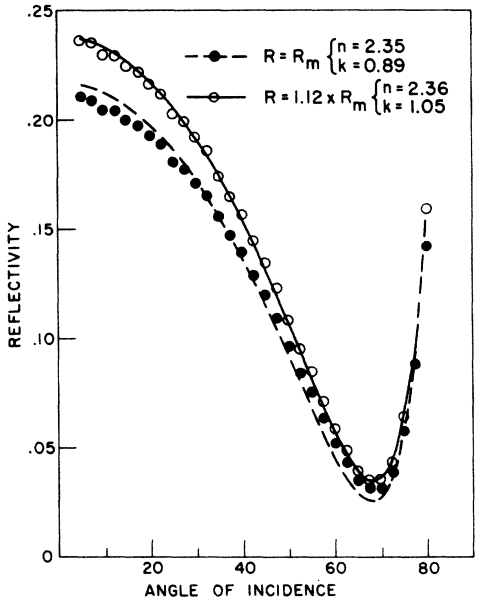

FIG. 3. Angular dependence of the reflectivity R_p for 4880-Å light polarized primarily along the C axis.

$$R_p = \left| \frac{N^2 \cos\varphi - (N^2 - \sin^2\varphi)^{1/2}}{N^2 \cos\varphi + (N^2 - \sin^2\varphi)^{1/2}} \right|^2 ,$$

where φ is the angle of incidence and $N = n + ik$. The optical anisotropy was therefore ignored in this fitting procedure, although data were taken with polarization both predominantly parallel and perpendicular to the C axis. This procedure gave a poor fit to the CrO_2 data, as is apparent from the lower curve and solid experimental points in Fig. 3, obtained for $\lambda = 4880$ Å. This problem is apparently due to a sizeable fraction of the incident light being diffusely reflected from irregularities in the CrO_2 film. If it is assumed that this scattered fraction of the incident light is independent of φ, the reflectivity values can be multiplied by a constant factor to improve the fit. The upper curve and the open circles in Fig. 3 illustrate the best fit obtained by this procedure for one CrO_2 sample after increasing the reflectivity values by 12%. A noticeably poorer fit was obtained when the reflectivity increase deviated from this optimum value by about 2%. Identical results were obtained for $\lambda = 6328$ Å. We have assumed that this diffuse scattering would not vary appreciably with wavelength, and the reflectance data for CrO_2 in Fig. 2 was increased at all wavelengths by this same factor. Although this assumption is open to question since the wavelength region of interest includes values comparable with the dimensions of inhomogeneities in the film, we feel that it is better than no correction at all.

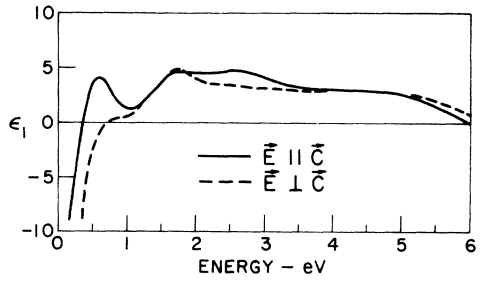

FIG. 4. Real part of the dielectric constant of CrO_2.

The Kramers-Kronig analysis was carried out by calculating the phase shift θ defined by $R = re^{i\theta}$ from the transform[9]

$$\theta(E) = \frac{E}{\pi}\int_0^\infty \frac{\ln R(E') - \ln R(E)}{E^2 - E'^2}\,dE' .$$

The optical constants n and k are then calculated by assuming normal incidence for the reflectivity measurements and using

$$n = 1 - R/(1 + R - 2\sqrt{R}\cos\theta),$$

$$k = 2\sqrt{R}\sin\theta/(1 + R - 2\sqrt{R}\cos\theta).$$

By varying the parameter p, the values of n and k, determined by angular-dependence measurements at two wavelengths, were least-squares fit to within 3% for CrO_2 with $p = 2.5$ and within 8% for MoO_2 with $p = 2.9$. In the latter case, the larger error is not understood, but it may result from our neglect of the anisotropy of the optical constants.

The dielectric constants determined from n and k are shown for CrO_2 in Figs. 4 and 5 and for MoO_2 in Fig. 6.

IV. DISCUSSION

Because there are no band-structure calculations for CrO_2 or MoO_2, the data can only be compared

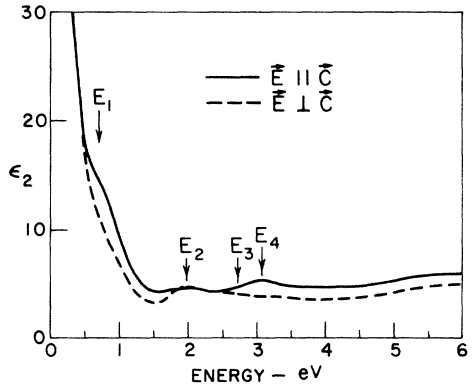

FIG. 5. Imaginary part of the dielectric constant of CrO_2.

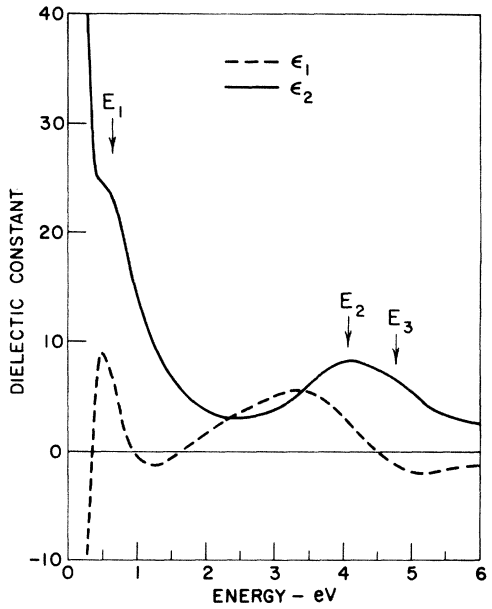

FIG. 6. Dielectric constants of MoO_2.

with that for VO_2 or TiO_2 to locate corresponding features, which have been interpreted for VO_2 on the basis of qualitative arguments concerning the nature of the band structure. This general picture[10] of the energy bands separates the d orbitals near the Fermi energy into two groups comprised of those t_{2g} orbitals with lobes in the basal plane of the rutile structure and those, denoted as $d_{\|}$, oriented along the C axis. The former orbitals π bond with the oxygen $2p$ orbitals to form a set of π^* bonds, while the latter are subject mainly to cation-cation overlap and may have either localized or itinerant character[10] depending on the cation separation along the C axis. In MoO_2, the $d_{\|}$ orbitals are assumed to be split by the monoclinic distortion with the lower level fully occupied by one of the $4d$ electrons per Mo^{4+}. The remaining electron is then in the π^* bands, so that one carrier per cation is expected. The ferromagnetic alignment in CrO_2 presumably leads to an exchange splitting of the $d_{\|}$ band, the lower level being fully occupied, and the remaining $3d$ electron per Cr^{4+} is again in the partially filled π^* bands. In metallic VO_2, it is possible that these d bands overlap, but it has been concluded that the $2p$ bands are below the lowest occupied $3d$ orbitals by about 2.5 eV. The evidence cited for this conclusion is the appearance of several absorption peaks above 2.5 eV accompanied by a steady rise in the absorption coefficient. The optical properties of CrO_2 are of the same general form with an absorption edge beginning at about 1.5 eV and a set of about three absorption peaks at $E_2 = 2$ eV, $E_3 = 2.7$ eV, and $E_4 = 3.1$ eV. The

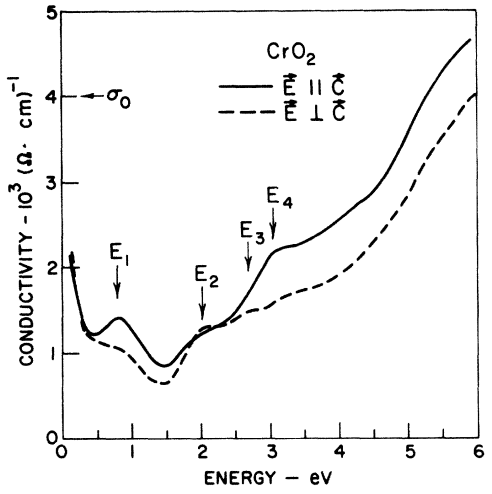

FIG. 7. Optical conductivity of CrO_2.

peak at E_3 is rather weak and is apparent only in the $E \perp C$ data. It is likely that these correspond to the transitions observed in metallic VO_2 at 2.9, 3.6, and 4.5 eV. This similarity is confirmed to some extent by the relative polarizations of these features in both materials, in that peaks at E_2 and E_4 are strongest in $E \perp C$ and $E \parallel C$, respectively.

Although less structure is found in the dielectric function of MoO_2 above 2 eV, the calculated absorption coefficient rises rapidly above 2.5 eV and peaks fairly sharply at 5 eV at $\alpha = 10^6$ cm^{-1}. There is a possibility of a double-peaked character to ϵ_2 in that region, denoted by $E_2 = 4$ eV and $E_3 = 4.7$ eV in Fig. 7. It may be concluded from these results that the lowest unfilled $4d$ levels in MoO_2 lie about 2.5 eV above the top of the $2p$ band.

The properties of both materials at energies up to 2 eV are dominated by the conduction electron response and a single absorption band, which leads to the shoulder in the reflectivity at low energies in Figs. 2 and 3. These two contributions to the optical properties are most clearly delineated in the real part of the conductivity, which is presented in Figs. 7 and 8, in which the measured dc conductivities are also given.

We have attempted to fit the free-electron contribution to the conductivity by a Drude response

$$\epsilon = \epsilon_\infty - [\omega_n^2/\omega(\omega + i\omega_c)].$$

However, the measurements on MoO_2 were not extended to $E \lesssim \hbar\omega_c$, and the CrO_2 measurements in that region may be questionable because of the correction made to account for the diffuse reflectivity and the conductivity peak at 0.8 eV. These fits to the conductivity data for CrO_2 give $\hbar\omega_n \sim 2.0$ eV and $\hbar\omega_c \sim 0.15$ eV. The dc conductivity calculated from these values and the relation $\sigma(0) = \omega_n^2/4\pi\omega_c$ is 3.6 $\times 10^3$ $(\Omega\,\mathrm{cm})^{-1}$, compared with the measured value[11] of 4×10^3 $(\Omega\,\mathrm{cm})^{-1}$ at 300 °K. After examining the effects of changing the corrections to the reflectivity on the fitted values of ω_n and ω_c, we feel that they are accurate to better than 30% for both ω_n and ω_c. If the number of carriers is assumed to be one per cation, this value of ω_n gives an effective mass ration $m^*/m_e \sim 10$ for CrO_2. Of course, only N/m^*, where N is the carrier density, is determined here. However, no data are available for either CrO_2 or MoO_2 from which N or m^* can be obtained separately. This assumption of one carrier per cation is made only for purposes of illustration.

Since the MoO_2 data does not extend to low enough energies, we have obtained a best fit to the data while requiring $\sigma(0)$ to be the measured dc value[12] of 10^4 $(\Omega\,\mathrm{cm})^{-1}$. This procedure gives $\hbar\omega_n \sim 2.7$ eV and $\hbar\omega_c \sim 0.1$ eV. The effective mass ratio obtained from these parameters and again assuming one carrier per cation is $m^*/m_e \sim 5$.

The peaks in the conductivities of both CrO_2 and MoO_2 at about 0.8 eV may be evidence that normal metallic conduction is not occurring. Shoulders in the reflectivities such as those which produced these peaks have also been observed in VO_2[2] and V_2O_3[13,14] and an absorption band at 1.0 eV has been reported[15] in Ti_2O_3. The optical conductivities of all these materials are not available, and we have found the absorption coefficients difficult to interpret because the calculated free-carrier absorption has a maximum at ~1 eV in all these materials. In fact, the absorption coefficients of CrO_2 and MoO_2 look quite different in this region due to the larger ω_n for MoO_2, whereas their conductivities are quite similar. Therefore, the reflectivities of VO_2 for $E \perp C$, V_2O_3, CrO_2 for $E \parallel C$, and MoO_2 are compared directly in Fig. 9 for $E < 2$ eV. The

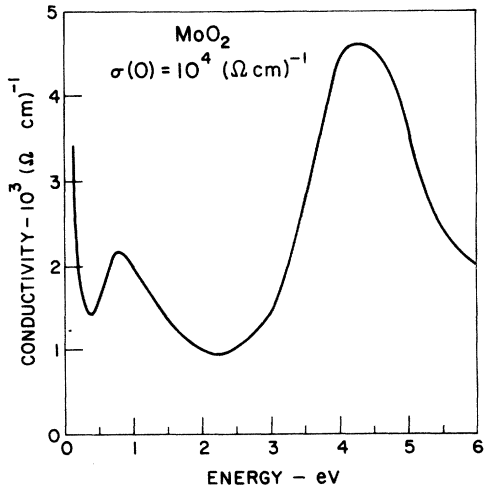

FIG. 8. Optical conductivity of MoO_2.

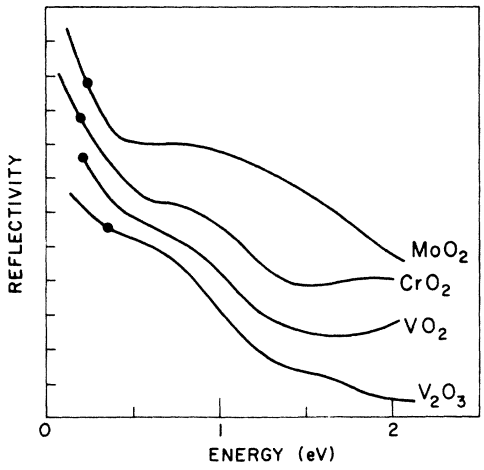

FIG. 9. Reflectivities of (a) MoO_2, (b) VO_2 ($E \perp C$), (c) CrO_2 ($E \parallel C$), and (d) V_2O_3. The VO_2 data are reproduced from Ref. 2, and the V_2O_3 data from unpolarized measurements by Fan (Ref. 14). The dot on each curve is at 70% reflectivity and the vertical divisions are at 10% intervals in reflectivity.

VO_2 data are from Ref. 3, and the V_2O_3 data are from unpolarized measurements of Fan.[14] Care must be taken in such direct comparisons of the reflectivity as is evident from the fact that the extension of the shoulder to higher energies in MoO_2 than in CrO_2 leads to an increase in the height of the 0.8-eV conductivity peak, but the shapes and positions of these peaks are almost identical.

The polarized measurements for VO_2 and CrO_2 differ in that the absorption shoulder appears only in $E \perp C$ for VO_2 and it is strongest in $E \parallel C$ for CrO_2. In other respects, the similarity of the spectra in this energy region is striking. In fact, oscillator fits to the VO_2 and V_2O_3 data give absorption bands at 0.74 eV for VO_2[3] and at 0.56 eV for V_2O_3. In previous investigations, these absorption peaks have been interpreted as interband transitions between the d bands. Conductivity peaks such as those at 0.8 eV in Figs. 7 and 8 are often observed in families of metals with identical crystal structures and conduction electron configurations, and have been explained in terms of transitions between the s bands.[16] This explanation is less likely in these oxides which differ in their structures and cation configurations, and crystal-field splittings might be expected to lead to a more complex and variable interband absorption spectrum. This is also apparent from the complexity of the calculated band structure for both phases of VO_2.[1] Although these qualitative arguments certainly do not exclude normal interband absorption as an explanation, there are two alternative mechanisms which might account for the presence of the similar absorption peaks near 1 eV in these materials.

A peak in the conductivity similar to that observed here is expected for Frank-Condon transitions from the ground state of a small polaron to the undistorted or free-carrier state. For temperatures above $\frac{1}{2}\Theta_D$, the conductivity has a peak at $E \sim 4U$, where U is the depth of the polaron well.[17] However, the conductivity at this peak is larger than the dc conductivity, in disagreement with the data presented here. There is a possibility that, if two types of carriers contribute to the conduction, both a Drude-like and small-polaronlike conductivity may result. Although it is unlikely that this two-band conduction would be found in so many materials, it has been suggested that the formation energy of a limited number of small polarons would be energetically favorable for a material near the Mott-Hubbard insulating limit.[18] At the present time, however, polaron absorption seems to be the least likely interpretation of the data since it would require small polarons, for which no firm evidence exists in these materials. However, this possibility could be checked by measuring the width of the 0.8-eV conductivity peak at higher temperatures.[17]

The second alternative is effectively an intraband absorption due to quasiparticle excitation for which the density of states is peaked at $E > 0$ when the intraion Coulomb energy U_c for double occupancy of a cation by electrons of opposite spin is comparable to, or greater than, the one-electron bandwidth W. The expected energy dependence of the conductivity has been examined recently using the Hubbard Hamiltonian and a tight-binding band in cubic symmetry.[19] It was found that the model predicted a Mott-Hubbard insulating state for $U_c > 0.8W$. In the metallic limit, $U_c < 0.8W$, the predicted conductivity has a shape similar to the peaks at 0.8 eV in Figs. 7 and 8 and a δ function at $E = 0$, which would become a Drude-like contribution for nonzero damping. The conductivity peak occurs at $E \sim U_c$, so that its position is a direct measure of the correlation energy in this model. The integrated conductivity obeys a sum rule,[19] which is a function of U_c. As U_c is increased, intensity is transferred from the free-electron response to the quasiparticle peak until an energy gap appears and the free-electron response vanishes. As $U_c \to \infty$, the integrated intensity decreases to zero. The experimental results for CrO_2 and MoO_2 would have roughly equal integrated intensities for the 0.8-eV peak and the Drude-like tail if it is assumed that the latter will approach the reported dc conductivities at low energies. The conductivity peaks could therefore be explained by $U_c \sim 1$ eV and $W \gtrsim 2$ eV, both of which are plausible estimates. For example, a recent estimate[20] of U_c from susceptibility data for VO_2 gives values the order of

1–2 eV. Further evidence of the plausibility of this model is the observation[19] that the quasiparticle absorption should have a similar shape in the insulating limit, although it is shifted slightly to higher energy for a given W. This agrees with the optical data for the semiconducting phases of VO_2 and V_2O_3, in which, in contrast with conventional semiconductors, a gradually increasing absorption is observed at low energies leading to a peak at $E \sim 1$ eV.[4,13]

A more quantitative test of this mechanism by fitting the data to the theory in its present form is not feasible. In addition to the uncertain applicability of the Hubbard model to realistic calculations of the density of states for $W \gtrsim U_c$, these materials have additional complications due to possibly overlapping bands, anisotropy, and in the case of CrO_2, a ferromagnetic alignment of both the $3d$ electrons per cation. However, none of these complications would appear to eliminate the explanation of the data on the basis of a correlation-perturbed density of states, since there are, in any case, an even number of electrons per cation.

CrO_2 may be useful in searching for further evidence of the nature of the 0.8-eV absorption. The increasing spin polarization as the temperature is passed through the Curie point may lead to substantial changes in U_c, which should be accompanied by changes in the shape and position of the 0.8-eV absorption.

V. CONCLUSIONS

We have found that the optical properties of CrO_2 and MoO_2 are consistent with a separation of the oxygen $2p$ states from the lowest unfilled d states of 1.5 and 2.5 eV, respectively. This p-d separation is about 3 eV in TiO_2 and 2 eV in VO_2, and the 1.5-eV separation for CrO_2 is therefore consistent with the trend, indicated by Wilson,[21] toward a decrease of this separation with increasing numbers of d electrons per cation. The free-carrier response has been fit by $m^*/m_e \sim 10$, $\hbar\omega_c = 0.15$ eV for CrO_2 and $m^*/m_e \sim 5$, $\hbar\omega_c \sim 0.1$ eV for MoO_2, assuming one carrier per cation in each case. The presence of similar peaks in conductivity at 0.8 eV in both materials may be related to quasiparticle absorption resulting from the alteration of the density of states by electronic correlation. If this interpretation of the data is valid, the position of this peak gives $U_c \sim 0.8$ eV for both CrO_2 and MoO_2. In that case the effective masses obtained from the data may be at least a factor of 2 too large, due to both the redistribution of the integrated conductivity from the free-electron response to the 0.8-eV absorption peaks and the decrease of integrated conductivity with increasing U_c.

ACKNOWLEDGMENTS

We appreciate the assistance of John Crane and Miss Karen Rutherford in performing the experiments.

---

†Work supported by the National Science Foundation Grant No. GH 33404.

[1]Ed Caruthers, Leonard Kleinman, and H. I. Zhang, Phys. Rev. B 7, 3753 (1973); Ed Caruthers and Leonard Kleinman, Phys. Rev. B 7, 3760 (1973).

[2]A. S. Barker, Jr., H. W. Verleur, and H. J. Guggenheim, Phys. Rev. Lett. 17, 1286 (1966).

[3]H. W. Verleur, A. S. Barker, Jr., and C. N. Berglund, Phys. Rev. 172, 788 (1968).

[4]Larry A. Ladd and William Paul, Solid State Commun. 7, 425 (1969).

[5]V. G. Mokerov and A. V. Rakov, Fiz. Tverd. Tela 11, 197 (1969) [Sov. Phys.-Solid State 11, 150 (1969)].

[6]B. S. Borisov, S. T. Koretskaya, V. G. Mokerov, A. V. Rakov, and S. G. Solovev, Fiz. Tverd. Tela 12, 2209 (1970) [Sov. Phys.-Solid State 12, 1763 (1971)].

[7]R. Srivastava and L. L. Chase, Solid State Commun. 11, 349 (1972).

[8]R. C. De Vries, Mater. Res. Bull. 1, 83 (1966).

[9]F. Stern, in *Solid State Physics*, edited by F. Seitz and D. Turnbull (Academic, New York, 1963), Vol. 15.

[10]John B. Goodenough, Prog. Solid State Chem. 5, 145 (1971).

[11]D. S. Rodbell, J. M. Lommel, and R. C. De Vries, J. Phys. Soc. Jpn. 21, 2430 (1966).

[12]D. B. Rogers, R. D. Shannon, A. W. Sleight, and J. L. Gillson, Inorg. Chem. 4, 841 (1969).

[13]A. S. Barker, Jr. and J. P. Remeika, Solid State Commun. 8, 1521 (1970).

[14]John C. C. Fan, thesis (Harvard University, 1972) (unpublished).

[15]W. J. Scouler and P. M. Raccah, Bull. Am. Phys. Soc. 15, 289 (1970).

[16]See, for example, N. V. Smith, Phys. Rev. 183, 634 (1969); J. G. Endriz and W. Spicer, Phys. Rev. B 2, 1466 (1970).

[17]H. G. Reik, in *Polarons in Ionic Crystals and Polar Semiconductors*, edited by Jozef T. Devreese (North-Holland, Amsterdam, 1972).

[18]N. F. Mott and Z. Zinamon, Rep. Prog. Phys. 33, 881 (1970).

[19]Ichiya Sadakata and Eiichi Hanamura, J. Phys. Soc. Jpn. 34, 882 (1973).

[20]C. J. Hearn and G. J. Hyland, Phys. Lett. A 43, 87 (1973).

[21]J. A. Wilson, Adv. Phys. 21, 143 (1972).